ISSN 0023-1584, Kinetics and Catalysis, 2007, Vol. 48, No. 4, pp. 589–598. © MAIK "Nauka/Interperiodica" (Russia), 2007.
Original Russian Text © E.A. Ustinov, V.B. Fenelonov, V.A. Yakovlev, P.I. Eletskii, 2007, published in Kinetika i Kataliz, 2007, Vol. 48, No. 4, pp. 629–638.

CARBON IN CATALYSIS

Characterization of the Porous Structure of Carbon Materials by Means of Density Functional Theory

E. A. Ustinov[a], V. B. Fenelonov[b], V. A. Yakovlev[b], and P. I. Eletskii[b]

[a] *NPO Provita, St. Petersburg, 199026 Russia*

[b] *Boreskov Institute of Catalysis, Siberian Branch, Russian Academy of Sciences, Novosibirsk, 630090 Russia*

e-mail: eustinov@mail.wplus.net

Received August 15, 2006

Abstract—Nitrogen adsorption isotherms were analyzed using density functional theory (DFT) to characterize active carbons. It is shown how the effect of technological parameters on the structure of active carbons can be revealed with the help of DFT. DFT is used to analyze the pore-size distribution and to determine the pore surface area for active carbons of different types.

DOI: 10.1134/S0023158407040180

Active carbons have found wide use as catalyst supports. The pore surface area and pore-size distribution in carbon materials have a profound effect on catalytic reactions. For this reason, carrying out a structural analysis of porous materials is a topical problem in the optimization of catalytic processes. Among the diversity of physical methods, the methods based on adsorption measurements are the most reliable for estimating pore structure parameters on the micropore and mesopore scales.

There are several adsorption-based approaches to the characterization of porous structure. The approaches of the first group include continual theories. One of them was proposed by Barrett, Joyner, and Hallenda (BJH) more than half a century ago [1]. The BJH method is based on the Kelvin equation for cylindrical pores and takes into account the thickness of the liquid films on their surfaces. The main disadvantage of this still popular theory is that it is thermodynamically incorrect. A liquid film adsorbed on the surfaces of pore walls is mechanically unstable because of the absence of a stabilizing adsorption potential. This is manifested as the fact that the grand thermodynamic potential corresponding to the basic equation describing capillary condensation is not minimal. A considerably more rigorous approach was developed by Broekhoff and de Boer (BdB) [2].

BdB theory is applicable to the pores of various geometries and can correctly describe the hysteresis phenomenon. Nevertheless, this theory has two essential limitations. First, the adsorbed film is treated as an incompressible liquid. Second, the adsorption potential was originally taken to be independent of the pore-surface curvature. However, these limitations have recently been eliminated [3, 4]. As a result, the nitrogen local isotherms calculated by the modified BdB method have benn reconciled with those calculated using nonlocal density functional theory (NLDFT) for the cylindrical pores with a diameter greater than 2 nm, i.e., for the entire range of mesopores. Similar results can also be obtained using the theory of Saam and Cole (SC) [5], although these authors proceeded from different assumptions. Another continual theory was suggested by Horvath and Kawazoe (HK) [6] for determining the porous structure in the micropore range. In spite of the fact that the HK theory has been successfully commercialized, this approach has some disadvantages because it does not take into account the change in the coordination number of the adsorbed molecule in a confined pore volume and treats adsorption as a usual condensation of bulk vapor in the external potential field produced by the pore walls. The attractiveness of the HK theory is in its ability to adequately describe experimental data. This is due to the fact that local adsorption isotherms have the shape of a Heaviside step function. Using a set of such step functions, one can accurately fit any experimental adsorption isotherm. The main limitation inherent in all continual approaches is that they are valid only for the mesopore range, i.e., for pores larger than 2 nm.

The theories of the second group are based on the molecular computations using various versions of the Monte Carlo [7–11] and molecular dynamics [12–14] methods. These methods are the most rigorous, but they are time-consuming. An alternative is DFT [15–19], which requires considerably fewer computational resources. This method reproduces well quantitative results obtained in numerical experiments. For this reason, DFT is applied here to the analysis of the pore-size distribution (PSD) and to the determination of the pore surface area, parameters of prime importance in catalysis.

BACKGROUND OF NONLOCAL DFT

Nonlocal DFT is based on the fundamental principle of minimizing the thermodynamic functional. For an open system, this functional can be written as

$$\Omega = \int \rho[f(\mathbf{r}, \rho, \bar{\rho}) + u^{\text{ext}}(\mathbf{r}) - \mu]d\mathbf{r}. \quad (1)$$

Here, ρ and $\bar{\rho}$ are, respectively, the local and smoothed densities; f is the Helmholtz free energy per molecule; u^{ext} is the external potential; and μ is the chemical potential. The Helmholtz free energy has three components. The first is the ideal-gas term $kT[\ln(\Lambda^3\rho) - 1]$; the second component is the Helmholtz free energy $f_{\text{ex}}(\bar{\rho})$ that takes into account only the intermolecular repulsive forces; and the third component involves the attractive potential $u(\mathbf{r})$ of intermolecular interaction. Thus, the Helmholtz free energy can be represented as

$$f(\mathbf{r}, \rho, \bar{\rho}) = kT[\ln(\Lambda^3\rho) - 1] + f_{\text{ex}}(\bar{\rho}) + u(\mathbf{r}), \quad (2)$$

where k is the Boltzmann constant and Λ is the de Broglie wavelength.

It is significant that the excess free energy is a function of the so-called smoothed density $\bar{\rho}$ rather than the local density ρ. That is why DFT is called nonlocal. The excess free energy is usually modeled using the Carnahan–Starling equation [20] for an equivalent gas of hard spheres of diameter d_{HS}:

$$f_{\text{ex}}(\bar{\rho}) = kT\frac{4\bar{\eta} - 3\bar{\eta}^2}{(1-\bar{\eta})^2}, \quad \bar{\eta} = \frac{\pi}{6}d_{\text{HS}}^3\bar{\rho}. \quad (3)$$

The smoothed density is a weighted average and includes the density gradient. The most popular approximation for the smoothed density was suggested by Tarazona [15]:

$$\bar{\rho}(\mathbf{r}) = \bar{\rho}_0(\mathbf{r}) + \bar{\rho}_1(\mathbf{r})\bar{\rho}(\mathbf{r}) + \bar{\rho}_2(\mathbf{r})(\bar{\rho}(\mathbf{r}))^2, \quad (4)$$

where

$$\bar{\rho}_i(\mathbf{r}) = \int \rho(\mathbf{r}')\omega_i(|\mathbf{r} - \mathbf{r}'|)d\mathbf{r}' \quad (5)$$

with $i = 0, 1, 2$. The functions $\omega_0(r)$, $\omega_1(r)$, and $\omega_2(r)$ are defined in such a way as to reproduce the direct correlation function for a hard-sphere gas [16], and they depend only on the distance r from a given point.

The component responsible for the attraction in the intermolecular potential is generally determined within the mean-field approximation:

$$u(\mathbf{r}) = \frac{1}{2}\int \rho(\mathbf{r}')\phi_{\text{ff}}(|\mathbf{r} - \mathbf{r}'|)d\mathbf{r}'. \quad (6)$$

Here, $\phi_{\text{ff}}(r)$ is the Weeks–Chandler–Andersen (WCA) pair attractive potential [21] derived from the Lennard-Jones 12-6 potential:

$$\phi_{\text{ff}}(r) = \begin{cases} -\varepsilon_{\text{ff}}, & r < r_{\text{m}} \\ 4\varepsilon_{\text{ff}}[(\sigma_{\text{ff}}/r)^{12} - (\sigma_{\text{ff}}/r)^6], & r_{\text{m}} < r, \end{cases} \quad (7)$$

where ε_{ff} and σ_{ff} are, respectively, the potential-well depth and the collision diameter of gas molecules, and $r_{\text{m}} = 2^{1/6}\sigma_{\text{ff}}$ is the coordinate of the potential minimum.

From the minimum thermodynamic potential condition, it follows that

$$\mu = kT\ln[\Lambda^3\rho(\mathbf{r})] + f_{\text{ex}}[\bar{\rho}(\mathbf{r})] + 2u(\mathbf{r}) + u^{\text{ext}}(\mathbf{r}) + \int \rho(\mathbf{r}')\frac{df_{\text{ex}}[\bar{\rho}(\mathbf{r})]}{d[\bar{\rho}(\mathbf{r}')]}\frac{\delta\bar{\rho}(\mathbf{r}')}{\delta\rho(\mathbf{r})}d\mathbf{r}'. \quad (8)$$

This equation accounts for the constancy of the chemical potential at any point of a confined volume for a given temperature and pressure in the bulk phase. The fact that the right-hand side of Eq. (8) is constant allows the density distribution to be found using a certain iteration scheme. After the density profile is found, the amount adsorbed can be found by integration:

$$a = \int \rho(\mathbf{r})d\mathbf{r}. \quad (9)$$

Thus, for a given pressure in the bulk phase, one can determine the amount adsorbed as a point on the adsorption isotherm.

However, to calculate the isotherm for a given pore size and shape, one must know the molecular parameters, the external (adsorption) potential, and the pore-size distribution. The first requirement can easily be solved using the properties of the bulk phase. Evidently, nonlocal DFT also applies to homogeneous fluids. Knowing the liquid and vapor densities at the saturation pressure, one can find at least two molecular parameters. The third parameter can be found from the known value of surface tension. The resulting parameters ε_{ff}, σ_{ff}, and d_{HS} can be used in a more complicated problem of determining the density distribution in the pore volume.

In many cases, the solid-fluid potential is known. For instance, the potential produced by the graphite surface is often described by the Steele equation [22]

$$u^{\text{ext}}(z) = 2\pi\rho_s\varepsilon_{\text{sf}}\sigma_{\text{sf}}^2\Delta \times \left[\frac{2}{5}\frac{\sigma_{\text{sf}}^{10}}{z^{10}} - \frac{\sigma_{\text{sf}}^4}{z^4} - \frac{\sigma_{\text{sf}}^4}{3\Delta(0.61\Delta + z)^3}\right], \quad (10)$$

where z is the distance at the graphite surface; ρ_s is the atomic density in graphite (114 nm^{-3}); Δ is the separation between the neighboring planes (graphenes) (0.335 nm); and ε_{sf} and σ_{sf} are the interaction parameters between the carbon atoms and adsorbed molecules.

For a slitlike pore, one should take into account the superposition of the potentials produced by the opposite walls.

Noncrystalline Surface

Conventional NLDFT was developed for crystal surfaces, such as graphitized carbon black. In these systems, the interaction potential between the adsorbed molecule and a solid has the shape of a narrow potential well. This leads to the formation of a nearly two-dimensional molecular layer on the surface at a distance corresponding to the potential-well minimum. If the density of this molecular layer is high enough, it becomes a source of the secondary potential field, resulting in the formation of the second molecular layer, and so on. As a consequence, this gives rise to a highly ordered layered structure of the adsorbed substance and to an almost step shape of the isotherm calculated for the sequential formation of molecular layers. At low pressures, the calculated isotherm always obeys the Henry law. However, in many cases, the experimental adsorption isotherms are rather smoothed, so that the Henry law is not observed in the pressure range accessible for measurements. It is most likely that, in these cases, one deals with a defective surface close to the surface of an amorphous solid. This is precisely the reason why the surface is energetically inhomogeneous and the linear portion of the experimental isotherm shifts to much lower pressures.

To take into account the defective surface structure, we have recently developed a new version of NLDFT [23–25]. Our approach is based on the interpretation of the Helmholtz free energy as a function of smoothed free volume rather than of density. This formulation does not lead to any changes in the description of the bulk phase or of the gas behavior at a distance from the surface. However, in the immediate vicinity of this surface, the smoothed free volume decreases due to the contribution from the atoms of a solid. This allows the repulsive potential arising between the solid and the adsorbed gas to be taken into account. The contribution of the attractive potential between the molecule and surface can be determined in a similar way, as was done for the intermolecular interaction within the framework of the WCA scheme [23]. However, more precise and informative results can be obtained by directly deriving the adsorption potential from the adsorption isotherm using the least-squares method [25]. In summary, we use the same ideology for both the intermolecular interaction and the solid-fluid interaction, because, in the case of amorphous structure of the solid, both media are disordered.

NITROGEN ADSORPTION ON NONPOROUS MATERIALS

Each method developed for the analysis of porous materials uses the surface of a reference nonporous body, either explicitly (BJH, BdB) or implicitly (numerical methods, NFDT). In the latter case, the reference surface is used for determining the interaction parameters between the molecules of adsorbed substance and atoms of a solid. For this reason, the proper choice of a reference system is an important component in the analysis of a porous structure.

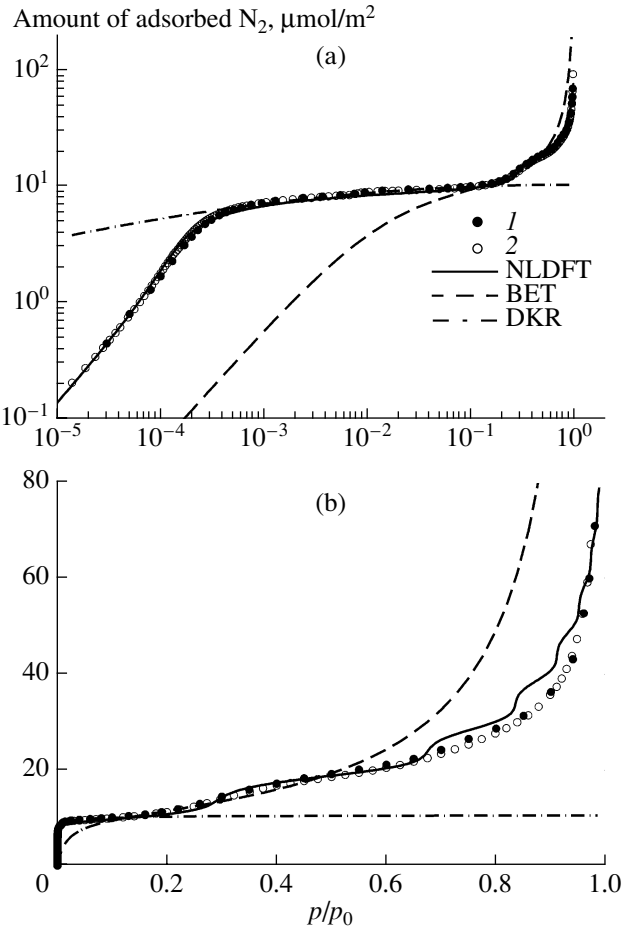

Fig. 1. (a) Logarithmic and (b) linear plots of the nitrogen adsorption isotherms on a graphitized carbon black at 77 K. The dots represent experimental data from (*1*) [26] and (*2*) [27], and the lines represent calculated data.

N_2 Adsorption on Graphitized Carbon Black

We apply NLDFT to nitrogen adsorption at 77 K on the surface of a graphitized carbon black as a representative of a crystalline solid. Figure 1 shows two, logarithmic (a) and linear (b), plots of the nitrogen isotherm at 77 K, according to data presented in [26, 27]. These isotherms fully coincide with one another, evidencing their high reliability. The dotted line is constructed according to the Brunauer–Emmett–Teller (BET) equation. One can see in Fig. 1 that the BET equation cannot adequately describe the experimental isotherm because of the too simplified model underlying this theory. Nevertheless, in most cases, excepting microporous systems, the BET method yields reasonable estimates for the surface area if the molecular area is chosen appropriately and if the range of relative nitrogen pressures is narrow enough (ordinarily from 0.08 to 0.3), so that the

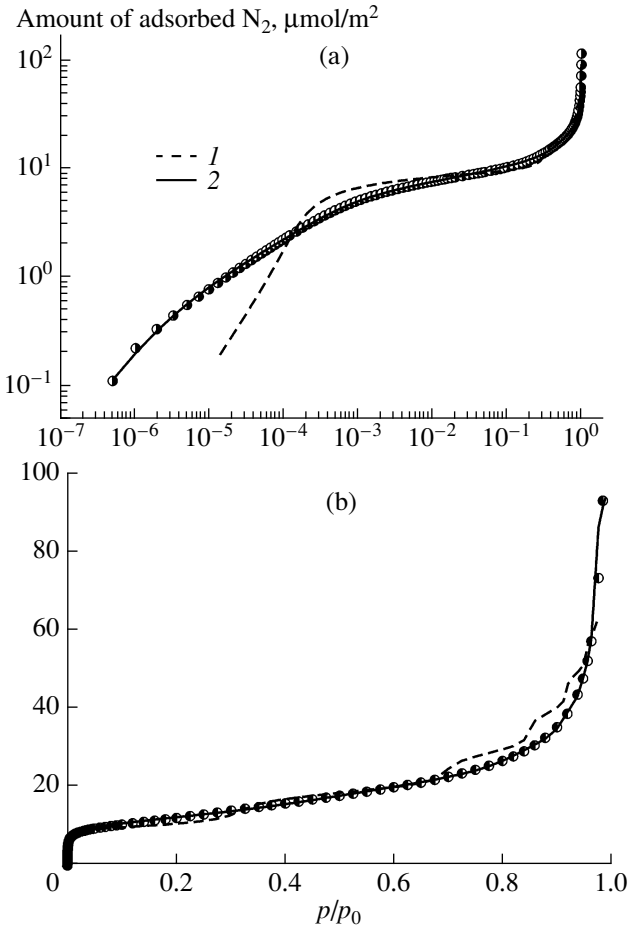

Fig. 2. (a) Logarithmic and (b) linear plots of the nitrogen adsorption isotherms on graphitized carbon black at 77 K [29]. Dots are for the experimental data, and lines are for the calculations using (*1*) original NLDFT developed for crystalline substances and (*2*) the new NLDFT version developed for amorphous solids.

BET equation can be linearized. The dot-and-dash curve is calculated by the semiempirical Dubinin–Kaganer–Radushkevich (DKR) equation [28]. In this case, the descriptive ability of the equation is also very poor. In particular, the calculated DKR isotherm does not reflect the Henry law in the low-pressure range and the following multimolecular adsorption after filling the first monolayer. In contrast to these simplified theories, the NLDFT calculation (solid line) adequately describes the experimental data in the pressure range covering five orders of magnitude. It should be emphasized that the carbon atom-nitrogen molecule interaction potential was the only adjustable parameter in the calculations.

N_2 Adsorption on Nongraphitized Carbon Black

The situation changes markedly for the case of adsorption on nongraphitized carbon black. The main distinction is associated with the presence of crystal defects and functional groups at the surface of a nongraphitized carbon black. The irregularities at the graphite surface make it similar to the microrough surface of an amorphous solid. Figure 2 shows the N_2 adsorption isotherm at 77 K on Cabot BP 280 nongraphitized carbon black [29]. The traditional NLDFT version developed for crystal surfaces gives appreciable deviations from the experimental adsorption isotherm (curve *1*), especially in the low-pressure range, where the calculated isotherm obeys the Henry law. The experimental isotherm is nonlinear at low coverage degrees because the defective microrough surfaces are energetically inhomogeneous, which is typical of noncrystalline solids. In contrast to the original NLDFT version, the new version perfectly describes the experimental isotherm (curve *2*). The contribution of the molecule–surface attractive potential was found directly from the isotherm by the method of least squares. This procedure allows one to gain detailed information on the adsorption potential and on its dependence on the chemical structure of the solid surface. In principle, the information contained in the potential curve can be further used for a more precise analysis of the interaction between the adsorbed molecules and a solid. This way is preferable to the attempts at predicting the potential using the empirical equations. From the practical point of view, the adsorption potential thus obtained can readily be used for modeling adsorption in variously shaped pores with allowance for the superposition of potentials produced by the opposite walls. The attractive potential obtained for the N_2–graphitized carbon black system is shown in Fig. 3 (curve *2*). Curves *3* in Fig. 3 represent the effective potential corresponding to original NLDFT for different pressures in the bulk phase. For a given relative pressure, the effective adsorption potential was determined in such a way that it gave the same density distribution of the adsorbed layer at the surface as did the calculation by the newly developed scheme. The increase of potential with pressure can be interpreted in the following way. At low pressures, molecules occupy the most active centers and thereby block them. For this reason, the subsequent sorption occurs on the less active centers. The sequential blocking of active centers leads to a decrease in the absolute value of the interaction potential between the nitrogen molecules and the surface. This signifies that the energetic inhomogeneity of a defective surface is "built" into the model. For comparison, the Steele potential derived for a crystalline graphite plate is also shown (curve *1*). Compared to the Steele potential, the effective potential is more complicated and has the form of a broader potential well.

What Carbon Black Should Be Used As a Reference?

Based on the data obtained, one can pose the question of what carbon black, graphitized or nongraphitized, should be used as a reference system in the analysis of the porous structure of carbon materials. Up to

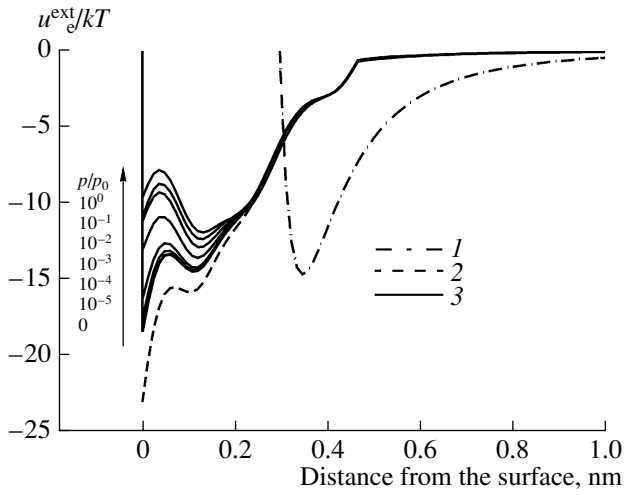

Fig. 3. Solid–fluid potential for the N_2 adsorption on Cabot BP 280 nongraphitized carbon black [29]: (*1*) potential corresponding to the surface of crystalline graphite, (*2*) attractive potential derived from the experimental isotherm by least squares, and (*3*) net potential for different pressures p/p_0.

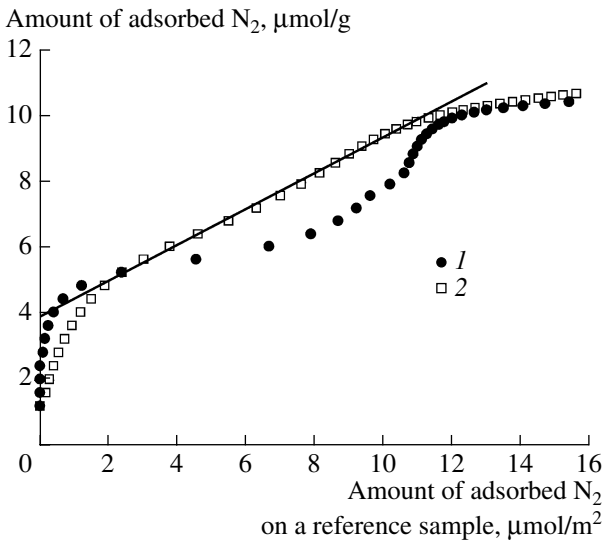

Fig. 4. Comparative plot of the N_2 adsorption on Norit activated carbon at 77 K. Reference samples: (*1*) graphitized carbon black and (*2*) Cabot BP 280 nongraphitized carbon black.

now, only graphitized carbon black has been used as a reference in the molecular computations and in NLDFT for the characterization of porous materials. This problem can be partially clarified by the data presented in the comparative plot representing the correlation dependence of the amount adsorbed on a porous material and the reference surface at the same pressures in the bulk phase (Fig. 4). It is presumed that, if the surface chemistry of both materials is similar, the correlation plot will exhibit the linear portion in a sufficiently broad pressure range, excluding the range of capillary condensation and filling micropores. Figure 4 presents the comparative plot of nitrogen adsorption at 77 K on active carbon Norit obtained from the coconut shell. One can readily see that, for the reference system of a graphitized carbon black, no linear segment is seen on the curve (dots *1*). However, a linear segment appears in the range of relative pressures from 10^{-4} to 0.1 upon replacing graphitized carbon black by nongraphitized carbon black (squares *2*). This situation is typical of the majority of active carbons and is indicative of a strong difference between the surfaces of pore walls in active carbons and the perfect basal graphite plane. This implies that, due to the presence of crystal defects and functional groups, the pore surface of active carbons is close to the surface of nongraphitized carbon black.

ADSORPTION IN PORES AND CHARACTERIZATION OF POROUS MATERIALS

Adsorption in Slitlike Pores

Once the isotherms for the surface of carbon black have been described, one can calculate the adsorption isotherm for the slitlike pores. To do this, one should account for the enhancement of the potential due to the superposition of the potentials from the opposite pore walls. In the case that the pore is large enough, the superposition effect is insignificant, so that the adsorption potential has two minima, and the adsorption on the opposite walls proceeds independently, as in the case of adsorption on the surface of a reference system up to the capillary condensation. As the pore width decreases, the potential strengthens and, eventually, two potential wells merge into one well. The potential strengthening results in the low-pressure shift of adsorption isotherms. A set of local nitrogen isotherms is presented in Fig. 5. For the pores with a width exceeding 1.1 nm, the isotherms have a vertical segment corresponding to the equilibrium phase transition. For the narrower pores, the effective critical temperature is lower than 77 K, and the phase transition is impossible, because the mean potential of intermolecular interaction lowers due to the decrease in the coordination number of molecules in a confined pore volume.

When analyzing the pore structure, one uses a considerably larger number of local isotherms covering the size interval up to 100–200 nm. Each local isotherm makes a contribution to the resulting isotherm. Therefore, the problem of determining the PSD function reduces to the determination of the weight coefficients for each of the local isotherms.

Deconvolution Problem

Let y be the function approximating the experimental isotherm, f be the required pore distribution, and ρ be the mean density of the adsorbed phase. Considering

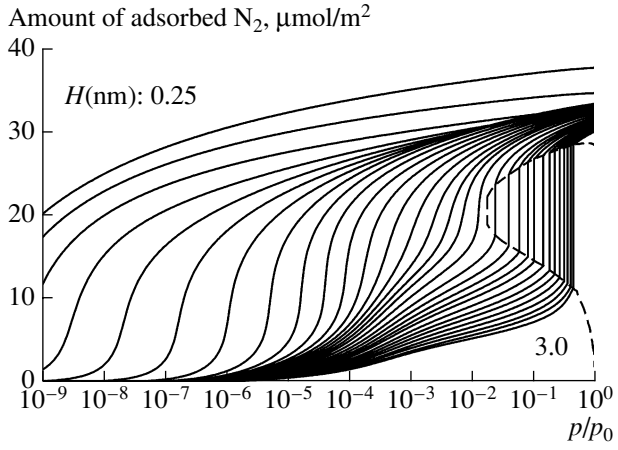

Fig. 5. Selected set of local nitrogen adsorption isotherms for slitlike pores with defective wall surfaces. Pore width H (from left to right, nm): 0.250, 0.298, 0.346, 0.393, 0.441, 0.489, 0.536, 0.584, 0.632, 0.679, 0.727, 0.775, 0.822, 0.870, 0.918, 0.965, 1.013, 1.085, 1.180, 1.275, 1.371, 1.466, 1.561, 1.704, 1.847, 1.991, 2.157, 2.348, 2.539, 2.753, and 2.992. The dotted line bounds the phase-transition region.

that ρ is a function of the pore width H and pressure p/p_0 in the bulk phase, y can be expressed as

$$y = \int f(H)\rho(p/p_0, H)\mathrm{d}H. \quad (11)$$

To find the distribution function $f(H)$, one should minimize the sum of deviations squared

$$\Re = \sum_i (y_i/a_i - 1)^2 + \alpha\varphi. \quad (12)$$

Here, i is the experimental point number, α is the parameter, and φ is a function to be defined below. In practice, the Fredholm integral in Eq. (11) is replaced by the sum of increments, so that, for $\alpha = 0$, the problem reduces to the calculation of a system of linear algebraic equations in volume increments. However, the result of deconvolution (which is known to refer to the class of ill-posed problems) is highly sensitive to experimental errors, especially if the number of partitions of the required function is large. Moreover, one can occasionally obtain physically unacceptable negative values for f. This problem was originally solved by Tikhonov in 1943 [30]. He developed the regularization (smoothing) method and introduced the "stabilizer" φ, as demonstrated in Eq. (12), where α is the regularization parameter. The stabilizer smooths the distribution function by suppressing insignificant peaks and dips. Below are two widely used stabilizer variants:

$$\varphi = \int\left(\frac{\mathrm{d}f}{\mathrm{d}H}\right)^2 \mathrm{d}H, \quad (13a)$$

$$\varphi = \int\left(\frac{\mathrm{d}^2 f}{\mathrm{d}H^2}\right)^2 \mathrm{d}H. \quad (13b)$$

The first of these equations corresponds to a set of "stretched springs" joining together the adjacent histogram vertices. These virtual springs accumulate elastic-strain energy. When released, such a system reduces its strain energy, leading to a decrease in the separation between the adjacent vertices and, respectively, to the smoothing of the distribution function. However, the standard deviation slightly increases. The balance of these two tendencies depends on the regularization parameter α. In the second case (Eq. (13b)), the stabilizer acts as an "elastic rod" resistant to bending.

In the general case, the stabilizer can be represented as

$$\varphi = \beta\int\left(\frac{\mathrm{d}f}{\mathrm{d}H}\right)^2 \mathrm{d}H - \int[-f\ln(f)]\mathrm{d}H - \lambda\int f\mathrm{d}H. \quad (14)$$

This equation resembles the grand thermodynamic potential that should be minimized. The parameter λ is introduced to suppress the insignificant peaks on the distribution function curve. The first term on the right-hand side of the equation can be considered as an analog of internal energy. The second term can be interpreted as information (Shannon) entropy serving as a measure of complexity for the system porous structure. The minimization of the functional ℜ requires an increase in entropy, i.e., simplification of the distribution function through the suppression of the prominent peaks and dips. One of the advantages of Eq. (14) is that the negative values of distribution function f cannot appear, because this equation includes the logarithm of f.

RESULTS

In this section, we consider two types of active carbons. The first of them is the representative of Sibunits, designed at the Boreskov Institute of Catalysis (Novosibirsk) and at the associated institutes of the Siberian Branch of the Russian Academy of Sciences [31]. Sibunits have a sponge structure; they are prepared by depositing pyrolysis products of a propane-butane mixture at 800–900°C on a granulated carbon black followed by the activation with CO_2 or H_2O. At the first activation step, the defective pyrocarbon clusters comprised of several graphenes are burned out to form micropores. At the second step, the carbon black particles are burned out, because their structure is less ordered. This process gives rise to relatively large voids. The nitrogen adsorption isotherm for 77 K is shown in Fig. 6. At pressures close to the saturation vapor pressure, the isotherm is very steep, evidencing the presence of rather large mesopores. The pore-size distribution obtained by NLDFT is shown in Fig. 7. Two peaks near 0.55 and 0.7 nm correlate with the micropores in pyrocarbon that was initially deposited on the surface of carbon black particles. Pores with a size of 2–3 nm are, most likely, the windows in pyrocarbon through which the activation products are expelled. The last broad peak with a maximum near 90 nm is due to a set of large voids appearing as a result of the burning out of carbon black particles. On the whole, the

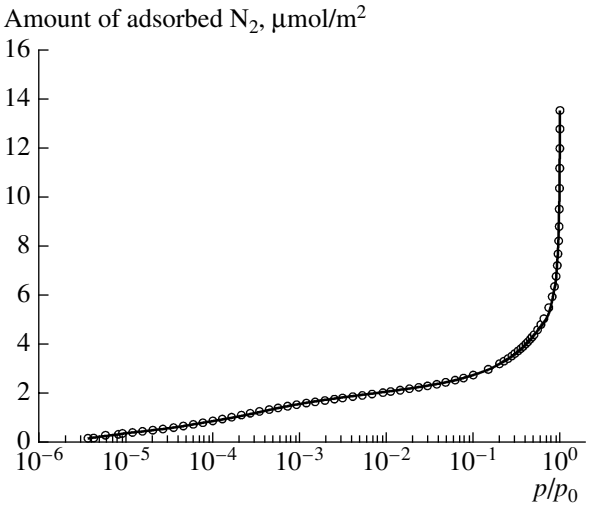

Fig. 6. Nitrogen adsorption isotherm at 77 K on a Sibunit activated carbon.

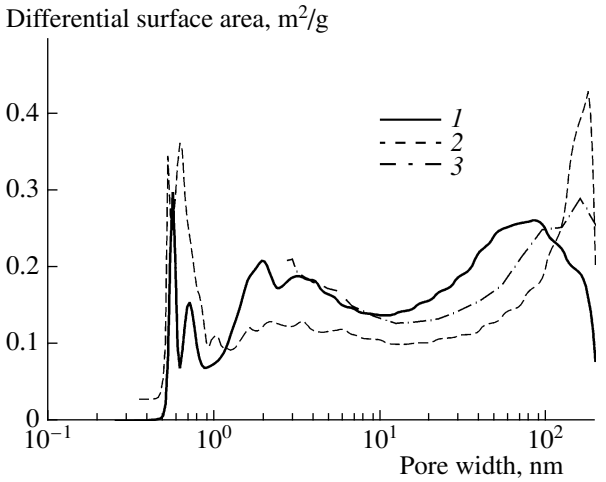

Fig. 7. Pore-size distribution function for Sibunit: (*1*) NLDFT and the regularization method, (*2*) Horvath–Kawazoe theory, and (*3*) BJH theory.

approach suggested in this work brought about precisely the structure that was anticipated for a Sibunit sample. For comparison, the pore distribution obtained by the Horvath–Kawazoe method is also shown in Fig 7 (curve *2*). One can see that the HK theory only qualitatively correlates with NLDFT. This is so because the HK theory does not take into account a change in the coordination number of molecules in narrow pores and does not transform asymptotically into the Kelvin equation for large pores. For this reason, the HK theory is unsuitable for the fine analysis of the structure of porous materials. The BJH calculation (curve *3*) yields better results in the mesopore range. The disparity is due to the fact that the BJH approach applies to the cylindrical pore model, whereas the NLDFT calculation is carried out for the slitlike model.

The second example is associated with the characterization of a set of nanostructural microporous carbons (NSMCs) obtained from rice husks by chemical activation at different temperatures. The nitrogen adsorption isotherms are presented in Fig. 8. The corresponding pore-volume and surface-area distributions are given in Fig. 9. One can see from Fig. 9 that there are four groups of pores in the carbons studied. An interesting regularity is that the micropore sizes do not change with increasing activation temperature, but the pore sizes of the fourth group increase markedly near the micropore-mesopore boundary. For an IUPAC value of 2 nm taken for this boundary, the mean size and the surface area of micropores decrease, while these characteristics increase with temperature for mesopores. Note that the total surface area of pores changes only slightly. However, a more detailed and adequate picture can be obtained from the individual analysis of each group. One can see in Fig. 10 that the size of all micropores remains almost unchanged, although the surface area and volume of the narrowest pores decrease, and, eventually, they disappear. This is most likely due to the pore blocking. The mean width and surface area of the largest pores gradually increase with temperature. These results are quite reasonable. And why are the sizes in two groups constant? The reason is that they arise after the chemical activation as a result of dissolving silica (ash) particles, which retain their size before dissolution. The total surface area is also presented as a function of activation temperature in Fig. 10b. For comparison, the total surface areas calculated by the comparative method discussed above (dotted curve) and by the BET method (dot-and-dash curve) are also shown in Fig. 10b. The comparative method yields reasonable results. By contrast, the BET method strongly overestimates the surface area. This

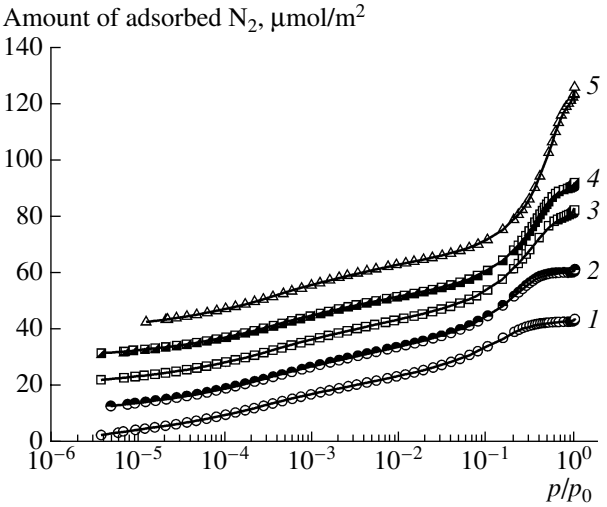

Fig. 8. Nitrogen adsorption isotherms on the NSMC samples obtained from rice husks by the chemical activation at different temperatures. For convenience, the isotherms are shifted up by 10 mmol/g along the ordinate axis for each subsequent activation temperature (°C): (*1*) 700, (*2*) 750, (*3*) 800, (*4*) 850, and (*5*) 900.

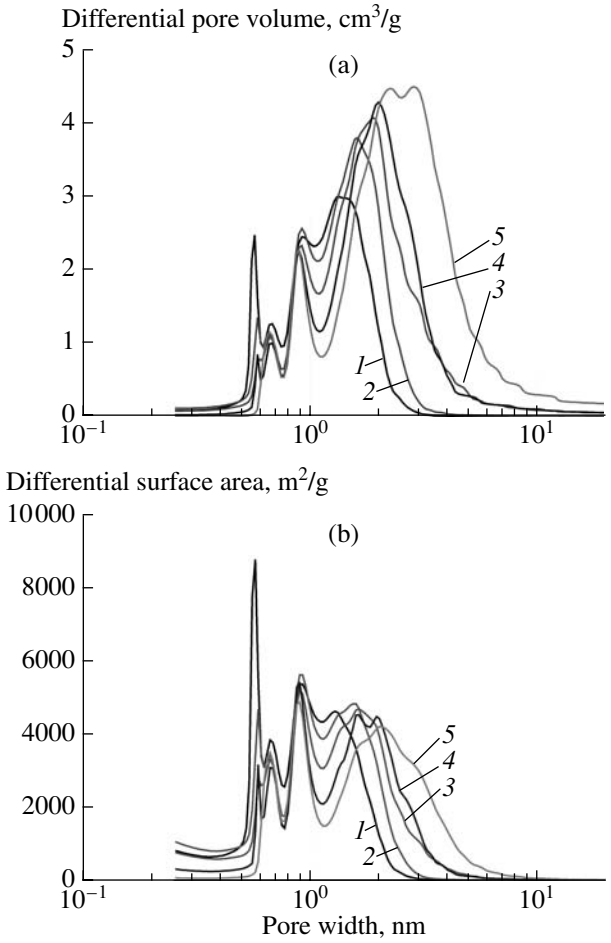

Fig. 9. (a) Pore-size and (b) surface-area distribution functions calculated using NLDFT for the NSMC samples obtained from rice husks by the chemical activation at different temperatures (°C): (*1*) 700, (*2*) 750, (*3*) 800, (*4*) 850, and (*5*) 900.

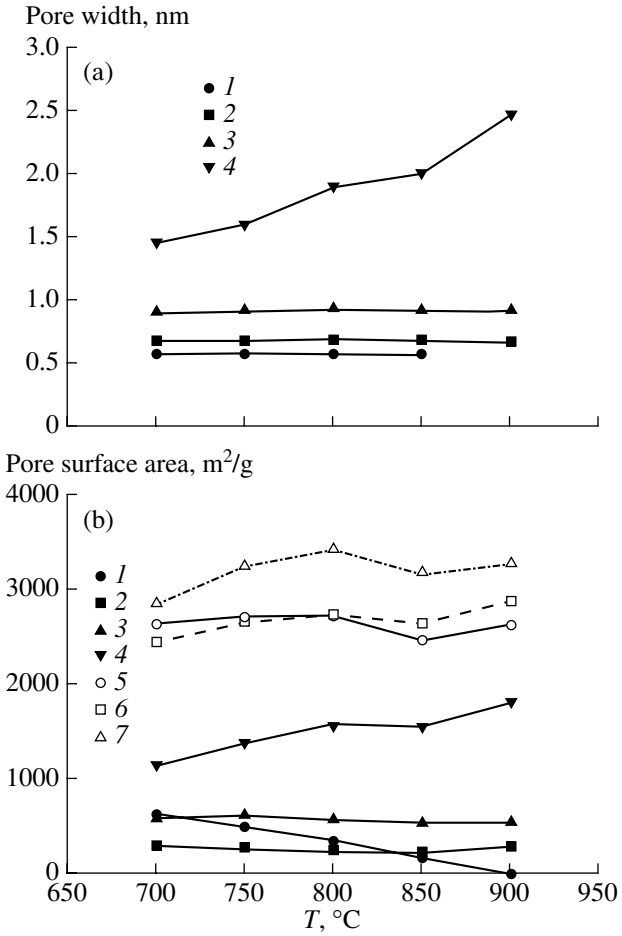

Fig. 10. Effect of the activation temperature (*T*) on the structure of NSMC samples: (a) pore width and (b) pore surface area. Pore groups: (*1*) micropores I, (*2*) micropores II, (*3*) micropores III, and (*4*) mesopores. The mean size of micropores is $H = 0.57$ (I), 0.67 (II), and 0.91 (III). The pore surface area is given separately for different groups. The temperature dependence of the total surface area is calculated by (*5*) NLDFT, (*6*) the comparative method, and (*7*) the BET method.

indicates that the BET method should not be used for estimating surface area in the microporous systems.

What Can an Analysis of PSD Contribute to the Study of H_2 Adsorption?

One of the intriguing problems is whether the information about the PSD extracted from the nitrogen adsorption isotherms can be used for analyzing the sorption of other gases, e.g., hydrogen? Figure 11 shows the hydrogen excess isotherms at 77 K for the same set of NSMCs as those considered in the preceding section. Because the changes in the volume of micropores and the surface area of mesopores with increasing activation temperature are considered above and known, one can carry out regression analysis with the aim of revealing a contribution from micropores and from the surfaces of broader pores to the overall H_2 excess adsorption. The regression equation can be written in the form

$$\Gamma = W_{\text{mi}}\Gamma_W + S_{\text{me}}\Gamma_S. \qquad (15)$$

Here, W_{mi} is the total volume of the three groups of micropores; S_{me} is the surface area of the fourth group that mainly includes mesopores. The purpose of our analysis is to find two universal isotherms corresponding to the adsorption in micropores and on the surface of mesopores. The isotherms obtained by simultaneously processing five hydrogen adsorption isotherms are shown in Fig. 12 separately for micropores (a) and mesopore surfaces (b). This provides important information on the relative contributions from the different groups of pores to the overall adsorption, which can be helpful in further attempts at synthesizing efficient adsorbents for storing hydrogen.

In summary, it is hoped that the method described in this work for the analysis of a porous structure will allow one to gain a deeper insight into the mechanism

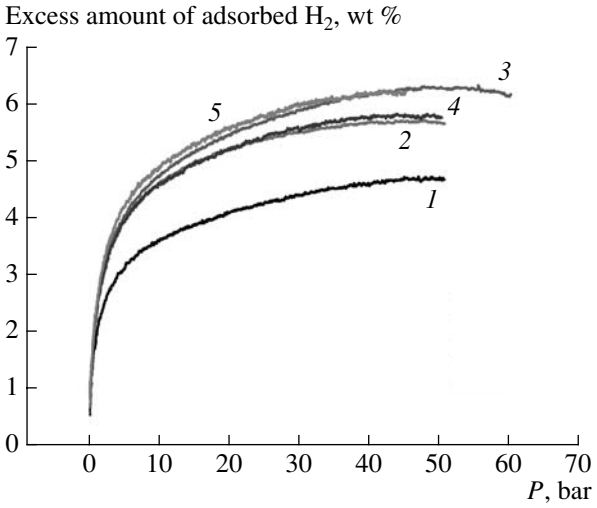

Fig. 11 Hydrogen excess adsorption isotherms at 77 K on the NSMC samples obtained for different activation temperatures (°C): (*1*) 700, (*2*) 750, (*3*) 800, (*4*) 850, and (*5*) 900.

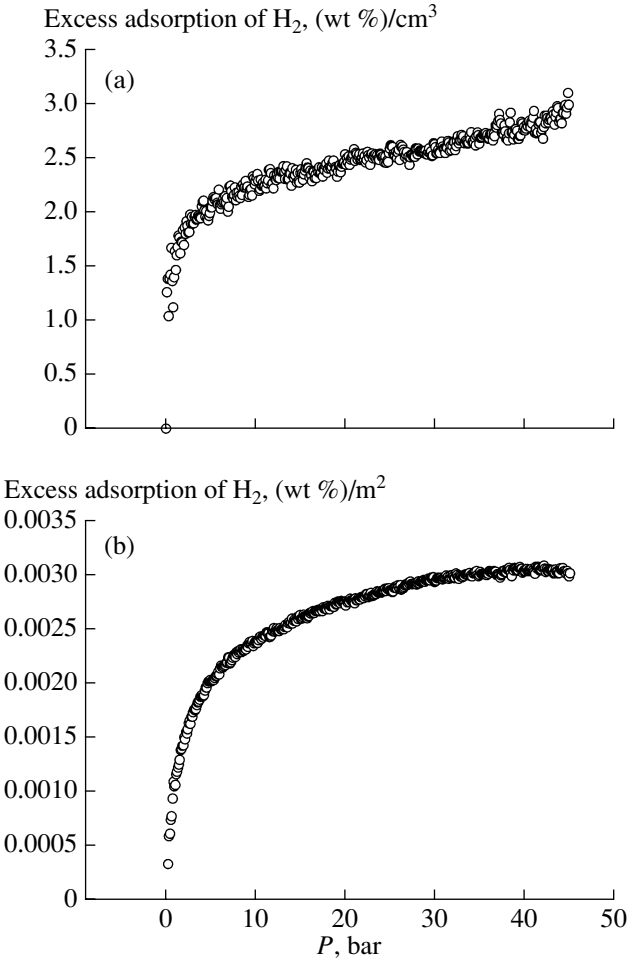

Fig. 12. Hydrogen excess adsorption isotherms (a) for micropores and (b) for the mesopore surfaces at 77 K, as determined by regression analysis using the pore volumes and surface areas derived from the nitrogen isotherms.

of structure formation and into the effect of technological parameters on the properties of porous materials.

CONCLUSIONS

The structure of pore walls in the majority of carbon materials is defective and close to the structure of the surface of nongraphitized carbon black. The new version of NLDFT takes into account a disordered structure of solid surfaces and can be used for the analysis of the porous structure of various porous materials and for the determination of their surface area and pore volumes. This approach allows one to trace the effect of technological parameters on the eventual structure of porous materials, which provides the possibility of synthesizing adsorbents and catalyst supports with desired characteristics. It has been shown that the porous structure derived from the nitrogen adsorption isotherms using NLDFT can be used in the analysis of hydrogen adsorption in micropores and on the surfaces of mesopores.

ACKNOWLEDGMENTS

This work was supported by the Australian Scientific Foundation and the Russian Foundation for Basic Research, project no. 06-03-32268-a.

REFERENCES

1. Barrett, E.P., Joyner, E.G., and Hallenda, P.P., *J. Am. Chem. Soc.*, 1951, vol. 73, p. 373.
2. Broekhoff, J.C.P. and de Boer, J.H., *J. Catal.*, 1967, vol. 9, pp. 8, 13.
3. Ustinov, E.A., Do, D.D., and Jaroniec, M., *J. Phys. Chem. B*, 2005, vol. 109, p. 1947.
4. Ustinov, E.A. and Do, D.D., *Colloids Surf., A*, 2006, vol. 272, p. 68.
5. Cole, M.W. and Saam, W.F., *Phys. Rev. Lett.*, 1974, vol. 32, p. 985.
6. Horvath, G. and Kawazoe, K., *J. Chem. Eng. Jpn.*, 1983, vol. 16, p. 470.
7. Lastoskie, C., Gubbins, K.E., and Quirke, N., *J. Phys. Chem.*, 1992, vol. 97, p. 4786.
8. Maddox, M.W., Olivier, J.P., and Gubbins, K.E., *Langmuir*, 1997, vol. 13, p. 1737.
9. Gelb, L.D., *Mol. Phys.*, 2002, vol. 100, p. 2049.
10. Vishnyakov, A. and Neimark, A.V., *J. Chem. Phys.*, 2003, vol. 119, p. 9755.
11. Coasne, B. and Pellenq, R.J., M, *J. Chem. Phys.*, 2004, vol. 120, p. 2913.
12. Nicholson, D. and Parsonage, N.G., *Computer Simulation and the Statistical Mechanics of Adsorption*, London: Academic, 1982.
13. Heffelfinger, G.S., van Swall, F., and Gubbins, K.E., *J. Chem. Phys.*, 1988, vol. 89, p. 5202.
14. Maddox, M.W., Quirke, N., and Gubbins, K.E., *Mol. Simul.*, 1997, vol. 19, p. 267.

15. Tarazona, P., *Phys. Rev. A: At., Mol., Opt. Phys.*, 1985, vol. 31, p. 2672.
16. Tarazona, P., Marconi, U.M.B., and Evans, R., *Mol. Phys.*, 1987, vol. 60, p. 573.
17. Ravikovitch, P.I., Wei, D., Chueh, W.T., Haller, G.L., and Neimark, A.V., *J. Phys. Chem. B*, 1997, vol. 101, p. 3671.
18. Ravikovitch, P.I. and Neimark, A.V., *Stud. Surf. Sci. Catal.*, 2000, vol. 129, p. 597.
19. Ravikovitch, P.I. and Neimark, A.V., *Colloids Surf., A*, 2001, vols. 187–188, p. 11.
20. Carnahan, N.F. and Starling, K.E., *J. Chem. Phys.*, 1969, vol. 51, p. 635.
21. Weeks, J.D., Chandler, D., and Andersen, H.C., *J. Chem. Phys.*, 1971, vol. 54, p. 5237.
22. Steele, W.A., *Surf. Sci.*, 1973, vol. 36, p. 317.
23. Ustinov, E.A., Do, D.D., and Jaroniec, M., *Appl. Surf. Sci.*, 2005, vol. 252, p. 548.
24. Ustinov, E.A., Do, D.D., and Fenelonov, V.B., *Carbon*, 2006, vol. 44, p. 653.
25. Ustinov, E.A., Do, D.D., and Jaroniec, M., *Langmuir*, 2006, vol. 22, p. 6232.
26. Isirikyan, A.A. and Kiselev, A.V., *J. Phys. Chem.*, 1961, vol. 65, p. 601.
27. Kruk, M., Li, Z., and Jaroniec, M., *Langmuir*, 1999, vol. 15, p. 1435.
28. Kaganer, G.M., *Dokl. Akad. Nauk SSSR*, 1952, vol. 116, p. 603.
29. Kruk, M., Jaroniec, M., and Bereznitski, Yu., *J. Colloid Interface Sci.*, 1996, vol. 182, p. 282.
30. Tikhonov, A.N., *Dokl. Akad. Nauk SSSR*, 1943, vol. 39, p. 195.
31. Fenelonov, V.B., *Vvedenie v fizicheskuyu khimiyu formirovaniya supramolekulyarnoi struktury adsorbentov i katalizatorov* (Introduction to the Physical Chemistry of the Formation of Supramolecular Structures of Adsorbents and Catalysts), Novosibirsk: Sib. Otd. Ross. Akad. Nauk, 2002, p. 310.